Turk J Elec Eng & Comp Sci, Vol.17, No.2, 2009, © TÜBİTAK
doi:10.3906/elk-0905-45

# CDM based controller design for nonlinear heat exchanger process

**Erkan İMAL**
*Department of Electrical and Electronics Engineering, Faculty of Engineering, Fatih University*
*Büyükçekmece, 34500, İstanbul-TURKEY*
*e-mail: eimal@fatih.edu.tr*

**Abstract**

*Most processes are nonlinear, and their control is a difficult yet important problem. The heat exchanger is an example one such nonlinear process. In the present paper, the effect of process nonlinearity on the performance of set point tracking and disturbance rejection in two controller methods is investigated. Initially, a first order plus dead time (FOPDT) model of the process is obtained via a software known as Loop-Pro Trainer. Then, the PI-controller tuning values are computed using the internal model control (IMC) correlations based on truncated (first-order) Taylor series approximation. Next, another controller is designed using the coefficient diagram method (CDM). Finally, the performances of the two controllers are compared. It is concluded that a more consistent performance is achieved with a CDM based controller in the environment of an exchanger process that is nonlinear with varying operating levels.*

**Key Words:** *Nonlinear process; Loop-Pro trainer; FOPDT model; PI-control; CDM.*

## 1. Introduction

A system is defined as linear if its input-output relationship satisfies superposition and homogeneity properties. In practice, as the variables increase beyond the linear range, nonlinearity arises. Thermal and fluidic processes are examples of nonlinear systems, and can be extremely difficult to control. For example, many variations of nonlinear behavior can cause the actuator to lose its influence under different operating conditions. Inherently nonlinear systems exhibit linear behavior in the vicinity of an operating point, and can be treated as a linear system. Then, one of many automatic control methods available for linear systems, such as conventional Proportional–Integral-Derivative (PID) controllers, can be effectively applied after linearization.

The PID controller is the most popular controller used in process control systems due to its remarkable effectiveness and simplicity of implementation. The technique is sufficient for the control of most industrial processes [1] and widely used. This controller has only three tuning parameters to be optimized, but their use is not simple. Thus, it is desirable to obtain a systematic procedure for tuning [2]. Controller performance for nonlinear processes will degrade whenever the measured process variable (PV) moves away from the design level of operation (DLO). This problem is demonstrated on a heat exchanger process running with a PI controller tuned for a moderate response and illustrated in Figure 1 [3]. Note that the nonlinear process behavior becomes apparent as the set point (SP) steps to higher temperatures. In the third SP step, from 170 °C to 185 °C, the same PI controller produces a different PV response, exhibiting more overshoot and slower damping oscillations than in the previous step.

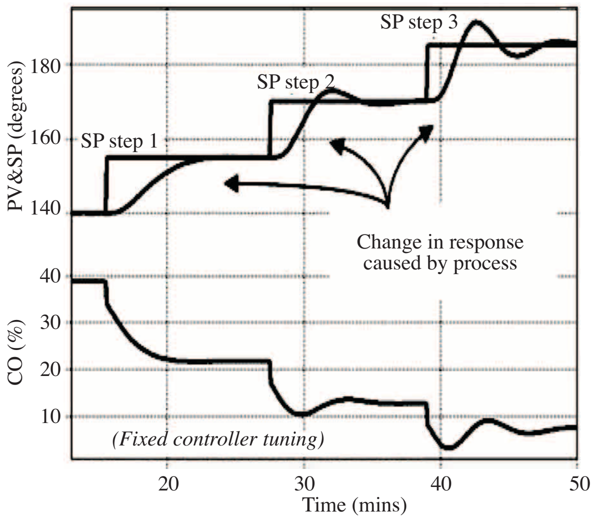


**Figure 1.** Controller performance degraded by nonlinear process behavior.

In the following, we review some studies on nonlinear process control. Huang et al. [4] presented a robust control method for a class of nonlinear systems, based on a mixed PID/adaptive algorithm. The nonlinear system is considered as a second-order linear dominant model with unmodeled dynamics which is possibly nonlinear and time-varying. The PID part of the controller is applied to stabilize the dominant model. The adaptive part of the controller is used to compensate for the deviation of the system characteristics from the dominant linear model for performance enhancement.

Bonivento et al. [5] investigated the problem of local output regulation of nonlinear systems in sliding mode terms, and showed that the controller solving the problem is the parallel connection of a dynamic linear system and a static nonlinear system. Their design methodology for an output feedback sliding mode regulator can be applied to both minimum and non-minimum-phase systems.

Cooper [6] proposed a parameter-scheduled adaptive controller. In this method, after having divided the total range of operation into a number of operating ranges, a controller algorithm (based on PID architectures) is selected for the application. Following the specification of loop sample time, the controller action (reverse or direct), and other design values, the tuning values are computed for the selected controller in each of the operating ranges every loop sample time. Thus, the controller continually adapts as the operating level changes to maintain a reasonably consistent control performance across a range of nonlinear behavior.

Another method is to use a polynomial approach as an appropriate and innovative solution, which is called the coefficient diagram method (CDM) proposed by Manabe [7, 8] initially for LTI systems, nonlinear systems for which performance changes with operating level. Many studies have been published on CDM applications in order to provide a desired performance in terms of the step response and disturbance rejection, hence an improved performance [9–18]. However, its potential to design controllers for nonlinear processes has not been entirely exploited yet. There are only a few publications that focus on CDM control of nonlinear plants [19].

In this paper, as an introduction to similar efforts in future studies, a CDM-based controller is used to control a nonlinear heat exchanger process, and its performance compared with that of the PI-controller. The PI-controller parameters and the FOPDT (i.e. First Order Plus Dead Time) model of the nonlinear process, which is considered for the CDM controller design, are obtained by using the software Loop-Pro produced by Control Station. The remainder of this paper is organized as follows: Loop-Pro software is introduced in Section 2. In Section 3, the FOPDT model is determined for the nonlinear heat exchanger process together with the best PI tuning values. In section 4, the coefficient diagram method is presented. In Section 5, a controller is designed using the CDM method for this process. In Section 6, the simulation results are given. Finally, the concluding remarks are drawn in section 7.

## 2. Loop-pro software

Loop-Pro is a software which has advanced graphical analysis tools for simulation-based studies in process control. These tools enable one to dynamically adjust the closed-loop time constant, and then to visualize changes in performance. In real-time, process performance can be interpreted in terms of set point tracking, robustness/stability, and other valuable measures.

The software is consists of three modules: *Case studies, Custom Process* and *Design Tools.* The *Case Studies* module includes a library of real-world process simulations developed using the data from actual processes, so their dynamics mirror real-world performance characteristics.

The *Custom Process* module is a block-oriented environment that lets the construction of a process and controller architecture with respect to desired specifications for a wide range of conventional control analyses. The benefits and drawbacks of different control architectures, tuning sensitivities, loop performance capabilities, and a lot of other important issues can be investigated.

The *Design Tools* module is used to fit linear models to process data by systematically searching for the model parameters that minimize the sum of squared errors (SSE) between the response contained in the measured data and the response predicted by the model, and then to compute PID controller tuning values. The obtained models can also be used to construct advanced control strategies which use process models internal to the control architecture [20, 21].

## 3. Modeling integrating (non-self regulating) processes

### 3.1. Heat exchanger

The heat exchanger, shown in Figure 2, is a counter-current, shell and tube, lubricating oil cooler. The measured process variable is lubricating oil temperature exiting the exchanger on the tube side. To maintain temperature, the controller manipulates the flow rate of cooling liquid on the shell side. The nonlinear dynamic behavior of the heat exchanger, or change in dynamic process behavior at different levels of the operating point is evident as seen in Figure 3. This is a significant issue to be considered in controller design [3].

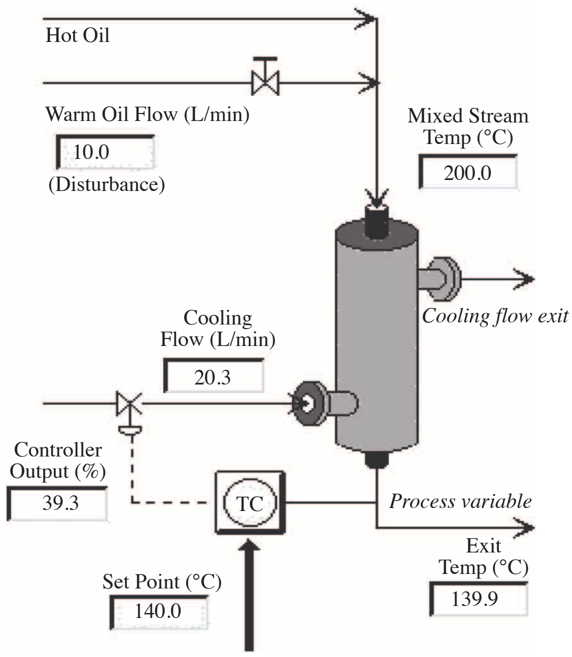


**Figure 2.** An example heat exchanger process with parameters.

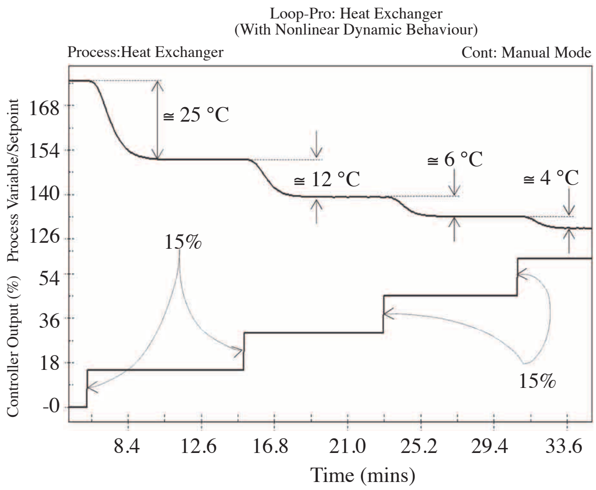


**Figure 3.** Nonlinear dynamic behavior of heat exchanger.

This process has a negative steady-state process gain (see Table 1); as the controller output (flow rate of cooling liquid) increases, the measured process variable (exit temperature) decreases. Another interesting point to be aware of is that changes in the flow rate of warm oil (disturbance) cause an inverse (non-minimum phase) response in the measured process variable (See Figure 4). That is, an increase in the disturbance flow rate causes the process variable to initially rise (due to faster flow), then decrease (due to cooler mixed liquid entering the exchanger), and eventually return to steady-state temperature.

**Table 1.** Model parameters suggested by the design tools.

| Model Parameters | | | |
|---|---|---|---|
| $K_p^*$ | $\tau_P$(min) | $\theta_p$(min) | SSE |
| -0.343 | 0.674 | 0.636 | 3.44 |

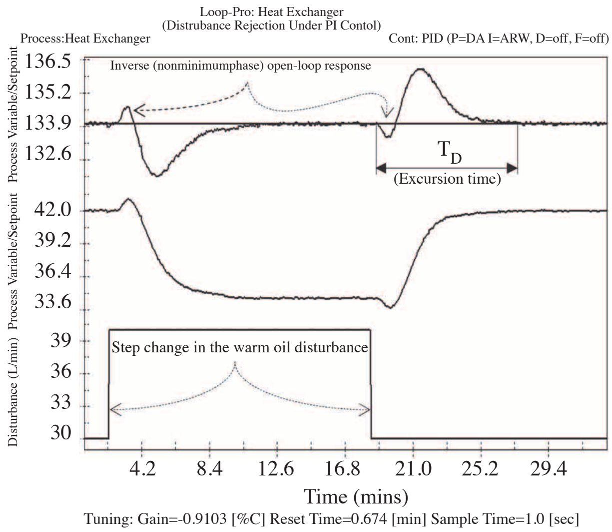


**Figure 4.** Non minimum phase response of heat exchanger to changes in disturbance under PI control.

## 3.2. Model determination for nonlinear process

The procedure for designing a controller in Loop-Pro software is as follows.

1. Move the process to the design level of operation and, when it reaches steady state, generate and collect dynamic data, i.e. the measured process variable response to change in the controller output. The typical values of the important disturbance variables should be determined and quiescently near those typical values.

2. Fit a first-order plus dead time (FOPDT) model to this data in *Design Tools.* In order to obtain a meaningful fit, it is essential to recognize the following limitations:

   - The process must be at steady state before collection of dynamic data begins, i.e. an exit temperature of 134 °C and a disturbance flow rate of 30 L/min.
   - The first data point in the file must equal this initial steady-state value.

   If these conditions are not met, the model fit will be incorrect, and of little value for tuning model based controller designs in simulation studies.

3. Use the resulting FOPDT model parameters in a correlation to compute initial PID controller tuning values. The tuning is performed using a well-known method of internal model control (IMC) correlations, which is an extension of the popular Lambda tuning correlations [22–24].

4. Implement the controller on the actual process and perform final tuning by trial and error until control objectives are satisfied.

Following the steps given above, the controller output is set at 42% to give the temperature of the exit stream at the design level of operation (DLO), which is considered to be 134 °C, and the warm liquid disturbance flow rate is expected to be about 30 L/min at the DLO. Using the doublet (two pulse tests amongst the others, such as pseudo-random binary sequence, step, pulse, sinusoidal, ramped) test in order to collect the test data in open-loop, the controller output value is changed from 42% up to 47%, then down to 37%, and finally back to its original value of 42%, as illustrated in Figure 5. Such a *doublet* test generates data both above and below the design level of operation, which is a desirable result when the process has a nonlinear characteristic. The process data are recorded in a file for process modeling and controller tuning studies.

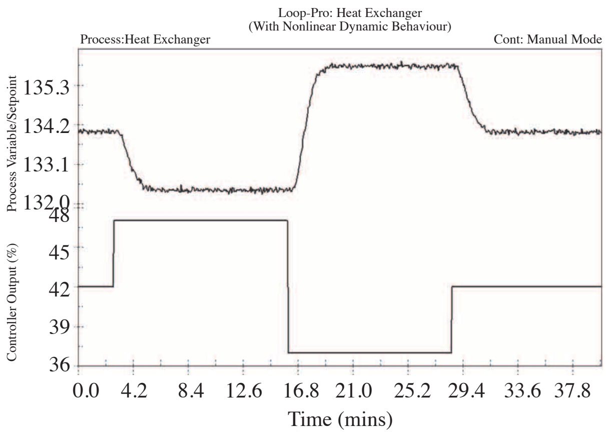


**Figure 5.** Dynamic process data generation through doublet test.

Since this process has a nonlinear characteristic, it is seen in Figure 3 that, although the change in the controller output is constant at each step of 15%, the measured exit temperature change is not the same for each step. This implies that the FOPDT model parameters, which are the steady state process gain $K_P$, the overall time constant $\tau_P$, and the apparent dead time $\theta_P$ will change as the operating level changes.

The FOPDT (overdamped) model describing the process behavior in time-domain and Laplace-domain is given in the equations

$$\tau_p \frac{dy(t)}{dt} + y(t) = K_p u(t - \theta_p) \tag{1}$$

$$\frac{Y(s)}{U(s)} = \frac{K_p e^{-\theta_p s}}{\tau_p s + 1}, \tag{2}$$

where $u$ is the input and $y$ is the output. The result of fitting FOPDT model to process data is shown in Figure 6. The model parameters computed by the *Design Tools* are also given in Table 1.

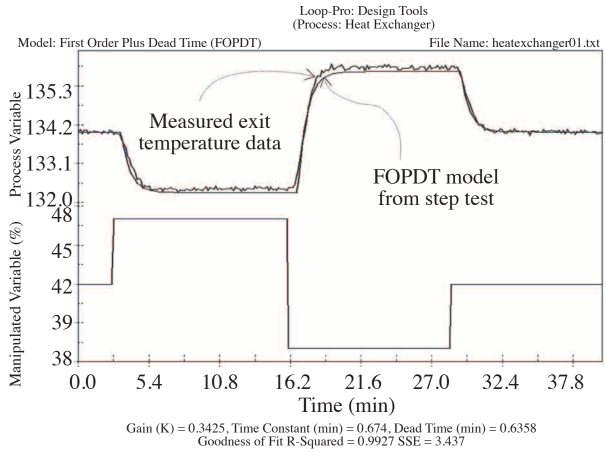


**Figure 6.** FOPDT model fit to dynamic process data.

Finally, substituting the model parameters given in Table 1 into equation (1) (or equation (2)) yields the FOPDT dynamic model describing the heat exchanger process behavior at this particular level of operation:

$$0.674\frac{dy(t)}{dt} = -0.343u(t - 0.636) \tag{3}$$

$$\frac{Y(s)}{U(s)} = \frac{-0.343e^{-0.636s}}{0.674s + 1} \tag{4}$$

## 3.3. Computing the PI tuning parameters

Using the IMC tuning correlations based on first-order Taylor series approximation ($e^{-\theta s} \cong 1 - \theta s$), the PI tuning parameters ($K_C$, controller gain and $\tau_I$, reset time) are computed for the heat exchanger process. The IMC PI tuning correlations for the process are given as [3]

$$K_C = \frac{1}{K_p}\left[\frac{\tau_p}{\tau_c + \theta_p}\right]; \qquad \tau_I = \tau_p. \tag{5}$$

The closed-loop time constant $\tau_C$ for the process is based on the process dead time and is given by
Moderate Tuning:

$$\tau_c = \left\{ \begin{array}{l} 8\theta_p \\ \tau_p \end{array} \right. \quad \text{whicheverislarger;} \tag{6}$$

Aggressive Tuning:

$$\tau_c = \left\{ \begin{array}{l} 8\theta_p \\ 0.1\tau_p \end{array} \right. \quad \text{whicheverislarger.} \tag{7}$$

Using the information given in equation (6) or equation (7), one set of tuning parameters $K_C$ and $\tau_I$ can be computed for this process using equations (5) and (6)

$$K_c = -0.344, \quad \tau_I = 0.674 \quad \text{min}. \tag{8}$$

The standard and aggressive PI tuning parameters suggested by *Design Tools,* and also the “Best” tuning parameters determined by trial and error approach are given in Table 2.

**Table 2.** Tuning parameters suggested by the design tools.

| Tuning Parameters | | | | | |
|---|---|---|---|---|---|
| PI Tuning Parameters[a] | | | PI Tuning Parameters[b] | | |
| $K_c$ | $\tau_I$ (mins.) | $\tau_c$ (mins.) | $K_c$ | $\tau_I$ (mins.) | $\tau_c$ (mins.) |
| -0.344 | 0.674 | 5.09 | -2.55 | 0.674 | 0.137 |
| [a] Dependent, Moderate Tuning (IMC tuning correlation)<br>[b] Dependent, Aggressive Tuning (IMC tuning correlation) | | | | | |
| “Best” PI Tuning Parameters by Trial and Error | | | | | |
| $K_c$ | $\tau_I$ (mins.) | $\tau_c$ (mins.) | | | |
| -0.910 | 0.674 | 1.53 | | | |

The suggested PI controller was implemented on the heat exchanger process, and its performance tested. Figure 7 shows the step response and disturbance rejection of the controller when the set point is stepped from 134 °C up to 144 °C, and after the response is complete (clear response is sufficient), back to 134 °C.

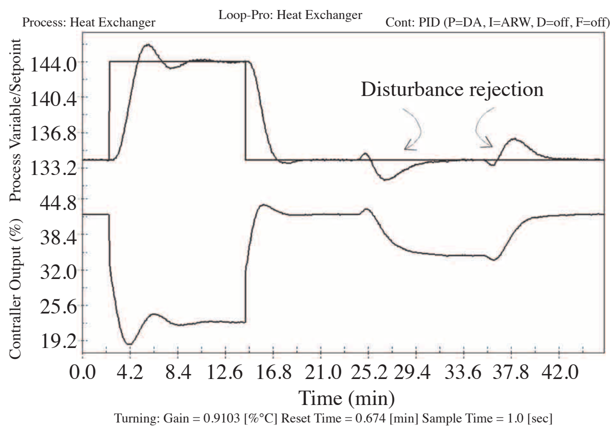


**Figure 7.** Step response and disturbance rejection of PI-controlled heat exchanger process.

The controller's disturbance rejection capability is also seen in Figure 7. It is tested through stepping the disturbance flow rate from 30 L/min to 40 L/min, and after the response is complete, back down to 30 L/min. If the controller tuning values that are best for the set point tracking does not appear to be the best for the disturbance rejection, trial and error method may be used to determine the best values for disturbance rejection. Eventually, the resulting tuning parameters satisfying both the set point and disturbance rejection requirements obtained by trial and error method may be averaged in order to get the "best" tuning values, i.e. $K_C$ and $\tau_I$. Thus, the best values are determined to give a set point tracking performance balancing a quick response with a modest overshoot and rapid decay. The response characteristics of the controller are given in Table 3.

**Table 3.** The response characteristics of a PI-controller.

| Moderate Tuning | | | |
|---|---|---|---|
| Stability Factor | Settling Time (min) | Percent Overshoot | CO Travel (%CO/hr) |
| 3.75 | 18.1 | N/A | 7.55 |
| IAE | | ITAE | |
| 5.62 | | 39.6 | |
| Aggressive Tuning | | | |
| Stability Factor | Settling Time (min) | Percent Overshoot | CO Travel (%CO/hr) |
| 1.38 | 6.59 | 34 | 24.3 |
| IAE | | ITAE | |
| 1.53 | | 5.58 | |
| "Best" Tuning by Trial and Error | | | |
| Stability Factor | Settling Time (min) | Percent Overshoot | CO Travel (%CO/hr) |
| 2.31 | 7.23 | N/A | 7.66 |
| IAE | | ITAE | |
| 2.16 | | 8.30 | |

To investigate the impact of the nonlinear behavior on controller performance using the best values of $K_C$ and $\tau_I$, the set point is stepped from 134 °C down to 124 °C, and back again. As for the disturbance rejection performance, it is stepped from 30 L/min down to 20 L/min and back to 30 L/min. The performances of the set point response and the disturbance rejection when compared to set point and disturbance increases, respectively, can be observed on Figure 8. Comparing Figures 7 and 8, it is seen that while the controller exhibits a different set point tracking performance in each case, the disturbance rejection performance remains the same. Another point to be aware of is that the controller output is saturated at 100%.

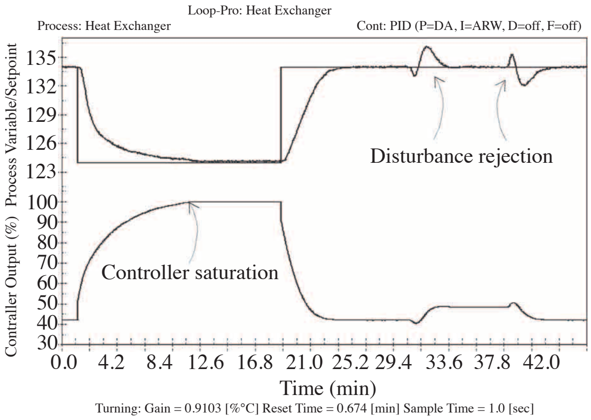


**Figure 8.** Effect of the nonlinear behavior on the step response and disturbance rejection of a PI-controlled heat exchanger process.

# 4. Coefficient diagram method

## 4.1. Introduction

When the denominator and numerator polynomials of a transfer function describing the input-output relationship of a linear time invariant (LTI) dynamic system are determined independently according to stability and response requirements, the design of the controller transfer function is not difficult except for the robustness issue. But this is also addressed by the coefficient diagram method (CDM) as well as others [7].

The CDM is an algebraic approach which simplifies the controller design process using the given characteristic polynomial, and gives sufficient information with respect to stability, response, and robustness in a single diagram. The CDM has three theoretical features: 1. The coefficient diagram, 2. The improved Kessler's standard form, and 3. The Lipatov's sufficient condition for stability.

When the plant dynamics and the performance specifications are given, one can find the controller under some practical limitations together with the closed-loop transfer function satisfactorily. As a first step, the CDM approach specifies partially the closed-loop transfer function and the controller, simultaneously; then decides on the rest of parameters by design. The parameters are stability index $\gamma_i$, equivalent time constant $\tau$, and stability limit $\gamma_i^*$, which represent the desired performance. The choice of the stability indices affect the stability and unsteady-state behavior of the system, and can also be used for the robustness investigation. As for the equivalent time constant, which specifies the response speed, hence the settling time [7].

## 4.2. Mathematical relations

In CDM, the characteristic polynomial is represented as in equation (9). This is also called as the target characteristic polynomial:

$$P(s) = a_n s^n + \cdots + a_1 s + a_0 = \sum_{i=0}^{n} a_i s^i. \tag{9}$$

The stability index $\gamma_i$, the equivalent time constant $\tau$, and the stability limit $\gamma_i^*$ are defined as

$$\begin{array}{l} \gamma_i = a_i^2/(a_{i+1}a_{i-1}); \quad i = 1 \sim n-1 \\ \tau = a_1/a_0 \\ \gamma_i^* = 1/\gamma_{i+1} + 1/\gamma_{i-1}; \quad \gamma_n = \gamma_0 = \infty. \end{array} \tag{10}$$

The coefficients in equation (9) are derived from equation (10) via the relations

$$\begin{array}{l} a_{i-1}/a_i = (a_j/a_{j-1})/(\gamma_i \gamma_{i-1} \cdots \gamma_{i+1}\gamma_j); \quad i \geq j \\ a_i = a_0 \tau^i/(\gamma_{i-1}\gamma_{i-2}^2 \cdots \gamma_2^{i-2}\gamma_1^{i-1}) = \frac{a_0 \tau^i}{\prod_{j=1}^{i-1} \gamma_{i-j}^j}. \end{array} \tag{11}$$

Then equation (9) can be expressed in terms of $a_0$, $\tau$, and $\gamma_i$ by the relation

$$P_{target}(s) = a_0 \left[ \left\{ \sum_{i=2}^{n} \left( \prod_{j=1}^{i-1} \frac{1}{\gamma_{i-j}^j} \right) (\tau s)^i \right\} + \tau s + 1 \right] \tag{12}$$

The equivalent time constant of the $i^{th}$ order $\tau_i$ and the stability index of the $j^{th}$ order $\gamma_{ij}$ are defined by the equation

$$\begin{array}{l} \tau_i = a_{i+1}/a_i = \tau/\left(\gamma_i \cdots \gamma_2 \gamma_1\right) \\ \gamma_{ij} = a_i^2/(a_{i+j}a_{i-j}) = \left[ \prod_{k=1}^{j-1} \left(\gamma_{i+j-k}\gamma_{i-j+k}\right)^k \right] \gamma_i^j \end{array} \tag{13}$$

$\tau$ is considered to be the equivalent time constant of the 0-th order, $\gamma_i$ to be the stability index of the $1^{st}$ order.

## 4.3. Stability condition

The sufficient condition for stability is given as [7][8].

$$\begin{array}{l} a_i > 1.12 \left[ \frac{a_{i-1}}{a_{i+1}} a_{i+2} + \frac{a_{i+1}}{a_{i-1}} a_{i-2} \right] \\ \gamma_i > 1.12\gamma_i^*, \quad for all i = 2 \sim n-2 \ . \end{array} \tag{14}$$

The sufficient condition for instability is

$$\begin{array}{l} a_{i+1}a_i \leq a_{i+2}a_{i-1} \\ \gamma_{i+1}\gamma_i \leq 1, \quad for some i = 1 \sim n-2 \ . \end{array} \tag{15}$$

### 4.4. Standard Manabe form

The recommended standard Manabe form of the stability index for an $n^{th}$-order system is expressed as

$$\gamma_{n-1} \sim \gamma_2 = 2, \qquad \gamma_1 = 2.5 \ . \tag{16}$$

This provides no overshoot in response to a step input for Type 1 system, but some overshoots for higher-type systems. The standard form yields the shortest settling time for the same value of $\tau$ for all types of systems, which is about $2.5\tau \sim 3\tau$.

### 4.5. Robustness consideration

The robustness concerns how fast the poles move to imaginary axis for the variation of parameters, and is only specified after the open-loop structure is specified. The robustness can be integrated into the characteristic polynomial with a small loss of stability and response. The condition may then be given as

$$\gamma_i > 1.5\gamma_i^*. \tag{17}$$

### 4.6. CDM design

The standard block diagram of Figure 9 is used in the CDM design process. The system output is given by

$$Y(s) = \frac{N_p(s)F(s)}{P(s)}R(s) + \frac{D_c(s)N_p(s)}{P(s)}D(s) \tag{18}$$

where $P(s)$ is the characteristic polynomial of the closed-loop system and is defined by

$$P(s) = D_c(s)D_p(s) + N_c(s)N_p(s) = \sum_{i=0}^{n} a_i s^i. \tag{19}$$

In equations (18) and (19), $R(s)$ and $D(s)$ are the reference input and the disturbance, respectively, $D_c(s)$ is the denominator of the controller transfer function, $F(s)$ and $N_c(s)$ are called the reference numerator and the feedback numerator of the controller transfer function, respectively. $N_p(s)$ and $D_p(s)$ are the numerator and denominator of the plant transfer function $G_p(s)$, respectively.

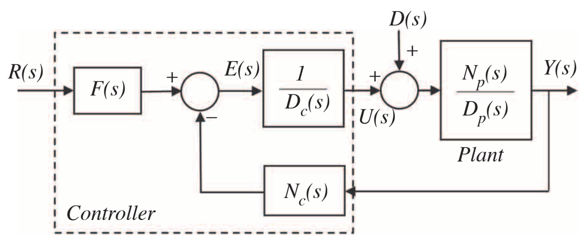


**Figure 9.** 2-DOF configuration.

When the performance specifications are given, they must be modified to the design specifications. In CDM, the design procedure is given in the following:

1. Define the plant in the right polynomial form.
2. Analyze the performance specifications and derive design specifications for CDM, i.e. $\tau$, $\gamma_i$, $\gamma_i^*$.
3. Assume the controller polynomials in the simplest possible form. Express it in the left polynomial form.
4. Derive the Diophantine equation, and convert it to Sylvester Form:

$$[C]_{nxn}\begin{bmatrix} l_i \\ k_i \end{bmatrix}_{nx1} = [a_i]_{nx1}; \tag{20}$$

   and solve for unknown variables. In equation 20, $C$ is the coefficient matrix, $l_i$ and $k_i$ are the controller design parameters, and $a_i$ are the coefficients of the target characteristic polynomial.
5. Obtain the coefficient diagram of the closed-loop system and make some adjustments to satisfy the performance specifications if necessary.

# 5. CDM controller design for heat exchanger

First Order Plus Dead Time (FOPDT) model is given for the heat exchanger process in equation (21) using the suggested parameters given in Table 2:

$$G_p(s) = \frac{Y(s)}{U(s)} = \frac{-0.343e^{-0.636s}}{0.674s+1} = \frac{N_p(s)}{D_p(s)}. \tag{21}$$

Using a simple Padé approximation for dead time in the Laplace domain, $e^{-\theta s} = {}^{2-\theta s}/_{2+\theta s}$, equation (21) becomes

$$G_p(s) = \frac{Y(s)}{U(s)} = \frac{0.22s-0.69}{0.43s^2+2s+2} = \frac{N_p(s)}{D_p(s)}. \tag{22}$$

It is considered that there is a step disturbance affecting the system. Thus, let the structure of the controller be chosen with $l_0$ =0 as follows:

$$G_c(s) = \frac{N_c(s)}{D_c(s)} = \frac{k_2s^2+k_1s+k_0}{l_2s^2+l_1s}, \tag{23}$$

where $l_2$, $l_1$, $k_2$, $k_1$, and $k_0$ are controller design parameters. Then, the closed-loop characteristic polynomial in terms of the controller design parameters (equation (19)) becomes

$$\begin{aligned} P(s) \; = \; & 0.43l_2s^4 + (2l_2+0.43l_1+0.22k_2)s^3 + (2l_2+2l_1-0.69k_2+0.22k_1)s^2 \\ & +(2l_1-0.69k_1+0.22k_0)s - 0.69k_0 \end{aligned} \tag{24}$$

The stability indices, and stability limits are determined to be $\gamma_i = [2, 2.25, 2.5]$, $\gamma_0 = \gamma_4 = \infty$, and $\gamma_i^* = \left[0.\overline{4}, 0.9, 0.\overline{4}\right]$, respectively. The stability index $\gamma_2$ is chosen different from the standard form of CDM in order to decrease the nonlinear effect on the time-response of the controlled system. Substituting them in equation (12) yields

$$P_{t\arg et}(s) = 0.234s^4 + 1.125s^3 + 2.704s^2 + 2.6s + 1. \tag{25}$$

Thus, setting equations (24) and (25) (the target polynomial) equal yields the Sylvester form in five unknowns. Then $l_i = [0.544, 0.668]$, and $k_i = [-1.14, -2.3, -1.45]$ are obtained for a settling time $t_s = 7.23$ min (see Table 3), i.e. $\tau$ =7.23/2.78 =2.6 min. $F(s)$ is obtained using the following expression in order to eliminate possible steady-state error in the response of the closed-loop system:

$$F(s) = \left. \frac{P(s)}{N_p(s)} \right|_{s=0} = k_0 \tag{26}$$

The semi-log coefficient diagram is depicted in Figure 10. In Figure 10, the coefficients, $a_i$, of the target characteristic polynomial (equation (9)), the stability indices $\gamma_i$, stability limits $\gamma_i^*$, and the equivalent time constant $\tau$, on the vertical logarithmic scales are plotted against the number of power of $s$ on the horizontal linear scale. The larger curvature of $a_i$ implies that the system is more stable which corresponds to larger stability index $\gamma_i$. Small equivalent time constant $\tau$ is indicated by the $a_i$ curve with its left side downwards, and implies swift response [7].

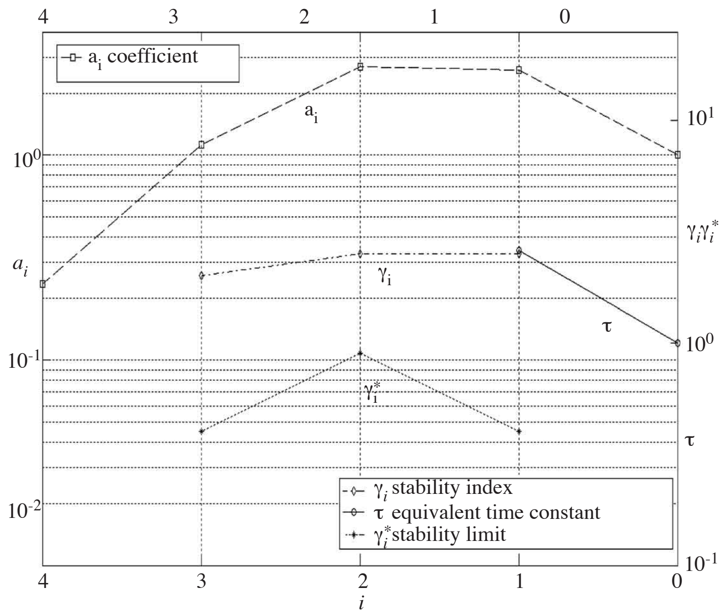


**Figure 10.** A plot of coefficient $a_i$ as a function of $i$.

## 6. Simulation results

The performance of the two controllers were compared by applying them to the same process. The step response, the disturbance rejection capability, and the root-locus diagram of the CDM-controlled heat exchanger process are shown in Figures 12–14, respectively. The results given in terms of the standard performance measures are presented in Table 4. Table 4 includes the impact of nonlinear behavior, as well. Table 4 shows that although the controller is PI, there is a steady-state error of 0.2 °C. This is because the controller output saturates at its upper limit, i.e. 100%, because of the process nonlinearity.

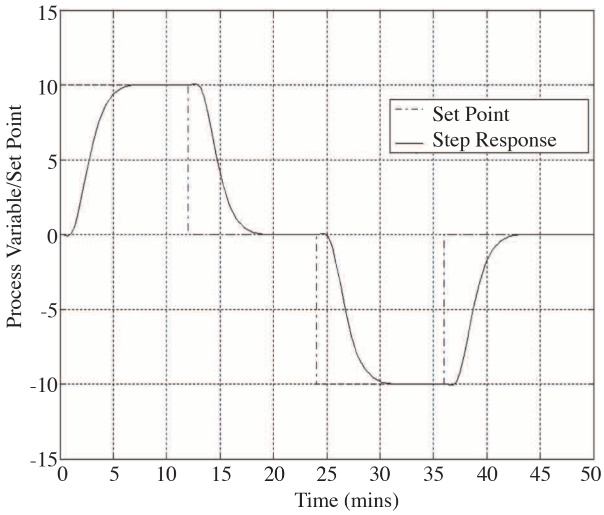


**Figure 11.** Step response of heat exchanger process (Controller Based on CDM).

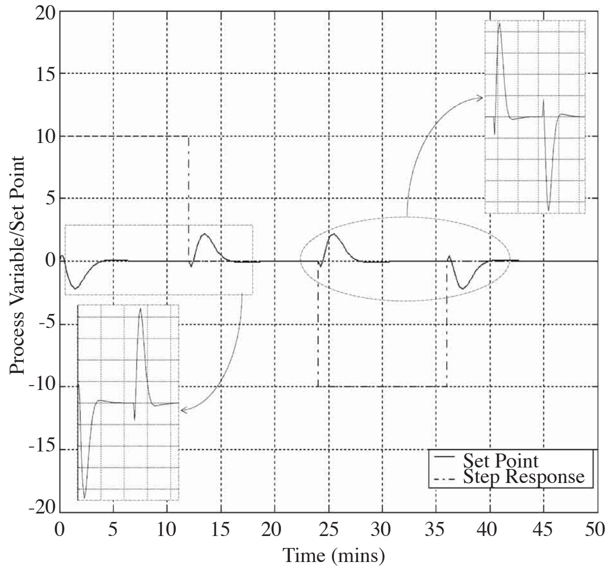


**Figure 12.** Disturbance rejection of heat exchanger process (Controller Based on CDM).

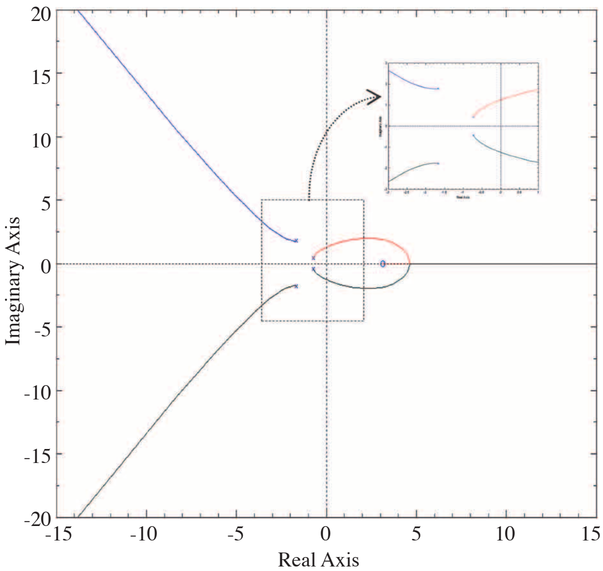


**Figure 13.** Root-locus diagram of heat exchanger process (Controller Based on CDM).

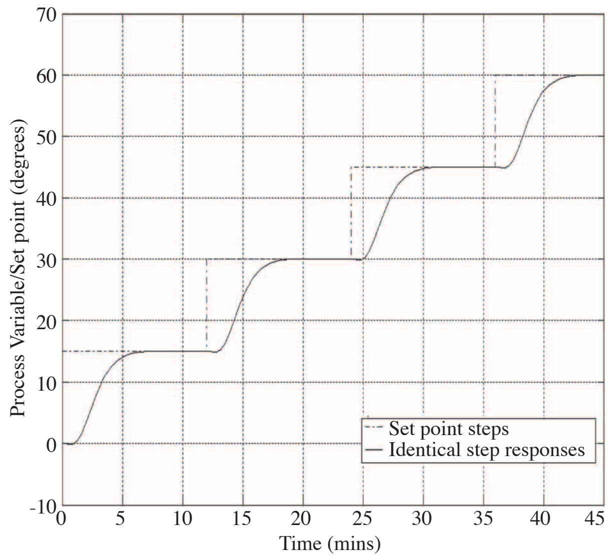


**Figure 14.** CDM controller performance under nonlinear process behavior.

The standard performance measures used in Table 4 are 10–90% rise-time $T_{r1}$; 0–100% rise time $T_r$; peak time $T_p$; settling time $T_s$(±2% band); percent overshoot, P.O.; and steady-state error $e_{ss}$. As it is seen the system is overdamped (no overshoot) in the case of CDM controller. Therefore, the peak time is not defined, and 0–100% rise time is not used. Thus, the controller performances should be evaluated with respect to $T_{r1}$, $T_s$, and $e_{ss}$. Overall, the PI-controlled system exhibits inconsistent responses as the set point is changed to upper and lower levels of the design level of operation. On the other hand, the CDM controller has better performance

**Table 4.** Time-domain performance characteristics.

| Heat Exchanger Process | | | | | | |
|---|---|---|---|---|---|---|
| Controller \ Criteria | $T_{r1}$ (mins) | $T_r$ (mins) | $T_p$ (mins) | $T_s$ (mins) | P.O. (%) | $e_{ss}$ (°C) |
| PI [(a)] | Set point stepped from 134 °C up to 144 °C | | | | | |
| | 1.41 | 2.56 | 3.54 | 6.73 | 18 | 0 |
| | Set point stepped back to 134 °C | | | | | |
| | 1.51 | 2.92 | 3.34 | 4.46 | 3 | 0 |
| PI [(b)] (study of nonlinearity) | Set point stepped from 134 °C down to 124 °C | | | | | |
| | 9.96 | - | - | 21.7 | - | 0.2 |
| | Set point stepped back to 134 °C | | | | | |
| | 6.3 | - | - | 10 | - | 0 |
| CDM[(c)] | Set point stepped from 0 up to 10 | | | | | |
| | 3.05 | - | - | 5.87 | 0 | 0 |
| | Set point stepped back to 0 | | | | | |
| | 3.00 | - | - | 5.94 | 0 | 0 |
| CDM[(3)] (study of nonlinearity) | Set point stepped from 0 down to -10 | | | | | |
| | 3.00 | - | - | 5.94 | 0 | 0 |
| | Set point stepped back to 0 | | | | | |
| | 3.00 | - | - | 5.94 | 0 | 0 |

[(a)] Determined from Figure 7; [(b)] Determined from Figure 8; [(c)] Determined from Figure 11

in terms of the shorter rise and settling times. Both controllers have zero steady-state error apart from one condition that the PI-controller was saturated after the set point had been stepped down to 124 °C, which caused an error of 0.2 °C. The disturbance rejection characteristics are given in detail in Table 5. The excursion time, negative peak and positive peak values are used to evaluate the disturbance rejection performances. The PI controller's performance in this regard is affected slightly by the nonlinear behavior of the process. As for the CDM controller, its disturbance rejection performance is not affected by nonlinearity, and is the same.

**Table 5.** Disturbance rejection characteristics.

| Heat Exchanger Process | | | |
|---|---|---|---|
| Criteria / Controller | Excursion time, $T_D$ (mins) | Positive peak of the error (°C) | Negative peak of the error (°C) |
| PI [(a)] | Disturbance stepped from 30 up to 40 L/min | | |
| | 9.1 | 0.7 | -2 |
| | Disturbance stepped back to 30 L/min | | |
| | 9.1 | 2.2 | -0.5 |
| PI [(b)] (study of nonlinearity) | Disturbance stepped from 30 down to 20 L/min | | |
| | 9.1 | 2.1 | -0.9 |
| | Disturbance stepped back to 30 L/min | | |
| | 9.1 | 1.3 | -1.9 |
| CDM[(c)] | Disturbance stepped from 30 up to 40 L/min | | |
| | 9.6 | 0.44 | 2.22 |
| | Disturbance stepped back to 30 L/min | | |
| | 9.6 | 0.41 | 2.22 |
| CDM[(c)] (study of nonlinearity) | Disturbance stepped from 30 down to 20 L/min | | |
| | 9.6 | 0.41 | 2.22 |
| | Disturbance stepped back to 30 L/min | | |
| | 9.6 | 0.41 | 2.22 |

[(a)] Determined from Figure 3 & 7 [(b)] Determined from Figure 8 [(c)] Determined from Figure 12

In contrary to Figure 1, the CDM controller performance for the nonlinear heat exchanger process remains the same even if the the set point (SP) steps continue to higher temperatures. This is shown in Figure 14.

## 7. Conclusion

In this paper, the performances of two controllers, a PI-controller and CDM controller, were investigated on the nonlinear heat exchanger process. As Figures 12–14 illustrate, a CDM controller can achieve consistent performance on the heat exchanger process that is nonlinear with changing operating levels. It has been shown that this method may be used in addressing such a difficult and important nonlinear control problem. If no overshoot together with the shorter rise and settling times is required out of the nonlinear heat exchanger process, the CDM based controller would be favorable. Moreover, it is also evident that the CDM-controlled system has better quality measure in rejecting a step disturbance compared with that of the PI-controller. Since the controller, $G_c(s)$, given equation (23) has an integrator term, the CDM controller performance is more consistent in terms of the excursion times, $\tau_D$, and the peak magnitudes of the disturbance error.

# References

[1] K. Åström, T. Hagglund, PID Controllers: Theory, Design and Tuning. USA, Instrument Society of America, 1995.

[2] S. Skogestad, "Simple analytic rules for model reduction and PID controller tuning", Journal of Process Control, Vol.13(4), pp. 291-309, 2003.

[3] D.J. Cooper, Practical Process Control, USA, Control Station, Inc., 2005.

[4] S.N. Huang, K.K. Tan, T.H. Lee, "A combined PID/adaptive controller for a class of nonlinear systems", Automatica, Vol. 37, pp. 611-618, Elsevier Science Ltd., 2001.

[5] C. Bonivento, L. Marconi, R. Zanasi, "Output regulation of nonlinear systems by sliding mode", Automatica, Vol. 37, pp. 535-542, Elsevier Science Ltd., 2001.

[6] Cooper, D. (2007). Parameter Scheduling and Adaptive Control of Nonlinear Processes. *Website of Control Station situated at* http://www.controlguru.com/2007/011107.html .

[7] S. Manabe, "Coefficient Diagram Method", 14*th* IFAC Symposium on Control in Aerospace, Seoul, Korea, pp. 199-210, 1998.

[8] S. Manabe, "Sufficient condition for stability and instability by Lipatov and its application to the CDM", $9^{th}$ Workshop on Astrodynamics and Flight Mechanics, Sagamira, ISAS, 1999.

[9] R.Hirokawa, K.Sato, S.Manabe, "Autopilot Design for a missile with reaction-jet using coefficient diagram method", AIAA Guidance, Navigation, and Control Conference and Exhibit, Paper 2001-4162, pp.1-8, Montreal, Canada, 2001.

[10] S.Manabe, "Application of coefficient diagram method to MIMO design in aerospace", IFAC 15th Triennial World Congress, pp. 1-6, Barcelona, Spain, 2002.

[11] I. Kaya, and M. Koksal. "Improving performance for a class of processes using coefficient diagram method", 9th IEEE Mediterranean Conference on Control and Automation, pp. 1-6, Dubrovnik, Croatia, 2001.

[12] S. E. Hamamcı, "A robust polynomial-based control for stable processes with time delay", Electrical Engineering, Vol. 87 (3), pp. 163-172, Springer Berlin, Heidelberg, 2005.

[13] Ö. Öcal, M.T. Söylemez, A. Bir, "Robust controller tuning based on coefficient diagram method", UKACC Control Conference, Control 2008, Paper ID: 147, pp. 1-6, Manchester, UK, 2008.

[14] S. Manabe, "The application of coefficient diagram method to the ACC benchmark problem", 2nd Asian Control Conference, II-135-138, Seoul, Korea, 1997.

[15] S. Manabe, “Application of coefficient diagram method to dual-control surface missile”, 15th IFAC Symposium on Automatic Control in Aerospace, pp.441-446, Bologna, Italy, 2001.

[16] Y.C. Kim, K. Kim, S. Manabe, “Sensitivity of time response to characteristic ratios”, IEICE Transactions Fundamentals, Vol.E89-A(2), pp. 520-527, 2006.

[17] M.S. Tavazoei, M. Haeri, “Comparison of the existing methods in determination of the characteristic polynomial”, Transactions on Engineering, Computing and Technology, pp. 130-133, 2005.

[18] M. Koksal, S.E. Hamamcı, “A program for the design of LTI control systems: CDMCAD”, Computer Applications in Engineering Education, Vol.12(3), pp.165-174, 2004.

[19] S. E. Hamamci, M. Koksal, S. Manabe, ”On the Control of some nonlinear systems with the CDM”, 4th Asian Control Conference, Singapore,2002.

[20] D.J. Cooper, User Guide Control Station 3.7 for Windows, USA: Control Station, Inc., 2004

[21] D.J. Cooper, Hands-on Workshop Series: A Companion to Practical Process Control Using LOOP-PRO 4.x. 73-76. USA: Control Station, Inc., 2004.

[22] Y. Li, K.H. Ang, G.C.Y. Chong, “Patents, software, and hardware for PID control”, IEEE Control Systems Magazine, pp. 42-54, February 2006.

[23] W.K. Woisznis, T.L. Blevins, D. Thiele, “Neural network assisted control loop tuner”, Proceedings of the IEEE International Conference on Control Applications, Vol.1, pp. 427-431, Kohala Coast-Island of Hawai, USA, 1999.

[24] K. H. Ang, G. Chong, Y. Li, “PID control system analysis, design, and technology”, IEEE Transactions on Control Systems Technology, Vol. 13, No. 4, pp. 559-576, July 2005.